

Enhanced resolution of marine viruses with violet side scatter

Yuan Zhao, Yanchu Zhao, Shan Zheng, Li Zhao, Wuchang Zhang, Tian Xiao, Gérald Grégori

▶ **To cite this version:**

Yuan Zhao, Yanchu Zhao, Shan Zheng, Li Zhao, Wuchang Zhang, et al.. Enhanced resolution of marine viruses with violet side scatter. Cytometry Part A, 2022, 10.1002/cyto.a.24674 . hal-03746755

HAL Id: hal-03746755
https://amu.hal.science/hal-03746755

Submitted on 7 Aug 2022

HAL is a multi-disciplinary open access archive for the deposit and dissemination of scientific research documents, whether they are published or not. The documents may come from teaching and research institutions in France or abroad, or from public or private research centers.

L'archive ouverte pluridisciplinaire **HAL**, est destinée au dépôt et à la diffusion de documents scientifiques de niveau recherche, publiés ou non, émanant des établissements d'enseignement et de recherche français ou étrangers, des laboratoires publics ou privés.



Distributed under a Creative Commons Attribution - NonCommercial - NoDerivatives 4.0 International License

Check for updates

Received: 8 October 2021 | Revised: 6 April 2022 | Accepted: 13 July 2022

DOI: 10.1002/cyto.a.24674

TECHNICAL NOTE

ISAC CYTOMETRY Journal of Quantitative Cell Science PART A

Enhanced resolution of marine viruses with violet side scatter

Yuan Zhao[1,2,3] | Yanchu Zhao[1,2,4] | Shan Zheng[2,3,5] | Li Zhao[1,2,3] | Wuchang Zhang[1,2,3] | Tian Xiao[1,2,3] | Gérald Grégori[6]

[1]CAS Key Laboratory of Marine Ecology and Environmental Sciences, Institute of Oceanology, Chinese Academy of Sciences, Qingdao, People's Republic of China

[2]Laboratory for Marine Ecology and Environmental Science, Pilot National Laboratory for Marine Science and Technology (Qingdao), Qingdao, People's Republic of China

[3]Center for Ocean Mega-Science, Chinese Academy of Sciences, Qingdao, People's Republic of China

[4]University of Chinese Academy of Sciences, Beijing, People's Republic of China

[5]Jiaozhou Bay Marine Ecosystem Research Station, Institute of Oceanology, Chinese Academy of Sciences, Qingdao, People's Republic of China

[6]Aix-Marseille University, Toulon University, CNRS, IRD, Mediterranean Institute of Oceanography UM110, Marseille, France

Correspondence
Gérald Grégori; Aix-Marseille University, Toulon University, CNRS, IRD, Mediterranean Institute of Oceanography UM110, Marseille 13288, France.
Email: gerald.gregori@univ-amu.fr

Funding information
2017-2019 Sino-French Cai Yuanpei Program; CNRS-NSFC Joint Research Projects Program, Grant/Award Number: CNRS-272110, NSFC 41711530149; International Research Project-Dynamics and Function of Marine Microorganisms (IRP-DYF2M); National Natural Science Foundation of China, Grant/Award Number: 42076139; Open Fund of Pilot National Laboratory for Marine Science and Technology (Qingdao), Grant/Award Number: QNLM20160RP0311

Abstract

Marine viruses make up an essential compartment of the marine ecosystem. They are the most abundant organisms and represent one of the biggest sources of unknown biodiversity. Viruses also have an important impact on bacterial and algal mortality in the ocean, and as such have a major influence on microbial diversity and biogeochemical cycling. However, little is known about the abundance and distribution patterns of viruses across the oceans and seas. Over the last 20 years, flow cytometry has been the technique of choice to detect and count the viral particles in natural samples. Nevertheless, due to their small size, the detection of marine viruses is still extremely challenging. In this article we describe how a new generation of flow cytometer which uses the side scatter (SSC) of violet photons from a 405 nm laser beam helps to improve the resolution for detecting marine viruses. To the best of our knowledge, this is the first report where virioplankton has been detected in aquatic samples using flow cytometry with a 405 nm violet SSC instead of a 488 nm blue SSC.

KEYWORDS
flow cytometry, 405 nm side scatter, sub-clusters, SYBR Green I, virus like particles

1 | INTRODUCTION

Viruses are the most abundant and genetically diverse life forms in the ocean. Estimates from direct counts of virus-like particles (VLPs) within seawater samples indicate that the global abundance of free viruses is at least 10^{30} individuals in the global ocean, translating into about 200 Mt of carbon [1]. Virioplankton could affect the marine biogeochemical cycle and energy flow by regulating the transfer and

Yuan Zhao and Yanchu Zhao have contributed equally to this work.

This is an open access article under the terms of the Creative Commons Attribution-NonCommercial-NoDerivs License, which permits use and distribution in any medium, provided the original work is properly cited, the use is non-commercial and no modifications or adaptations are made.
© 2022 The Authors. *Cytometry Part A* published by Wiley Periodicals LLC on behalf of International Society for Advancement of Cytometry.

transformation of organic matter in the marine microbial food web [2].

Detection and accurate, reliable enumeration of virioplankton is critical for providing essential information about virus abundance, distribution, production and decay, and understanding their ecological function in marine biogeochemistry [3, 4]. Abundant VLPs within aquatic environments were discovered about 30 years ago, using transmission electronic microscopy (TEM) [5–7]. TEM provides information on the shape and size of VLPs, however, it is expensive, time consuming and lacks precision [2]. With the development of DNA-binding fluorescent stains such as DAPI (4′,6-diamidino-2-phenylindole), SYBR Green I, SYBR Gold, and Yo-Pro-1 as well as high porosity aluminum oxide anodisc filters (0.02 μm pore size), scientists started to enumerate VLPs using epifluorescence microscopy (EFM) [8, 9]. EFM is cheaper and comparatively faster than TEM, whereas it is difficult to discriminate large VLPs from small bacteria, leading to counting errors [2].

Over the past three decades, flow cytometry (FCM) has proven to be useful in the field of marine environmental microbiology [10–12], and has led to some fundamental changes in our understanding of the marine biogeochemical cycles and energy flow [13]. The smallest photoautotroph known to date is *Prochlorococcus*. It is the numerically dominant primary producer in open ocean ecosystems and was discovered by flow cytometry [12]. FCM allows fast analysis of individual cells/particles according to their light scatter properties and fluorescence characteristics, providing quantitative information of marine pico- and nanoplankton [14] as well as virioplankton [15]. FCM has become the preferred method for quantifying VLPs in aquatic samples due to its advantage in terms of speed, accuracy and cost [4].

Since the first report using FCM to quantify the abundance of VLPs in natural seawater [16], there have been a large number of publications on this subject. Most of the researches use the nucleic acid dye SYBR Green I (Molecular probes, Eugene, OR), which emits a broad fluorescence upon excitation with a 488 nm (blue) laser beam, reaching a maximum at the green wavelength (530 nm) with a high fluorescence yield [15]. VLPs are identified on the bi-parametric plot defined by the right angle blue side scatter (BSSC) versus the green fluorescence of SYBR Green I [15]. According to the literature, in natural seawater samples, virioplankton can usually be divided into 2 or 3 sub-populations on the basis of their relative green fluorescence intensity [15, 17–19].

A recent study suggests that the 405 nm violet side scatter (VSSC) being a shorter wavelength could be superior to BSSC in detecting metal nanoparticles. Indeed VSSC yielded smaller coefficient of variations (CVs) and a greater separation index (SI) compared with blue light excitation [20]. SI was measured using the means and standard deviations (SD) of two smaller bead peaks (e.g., 200 and 300 nm) [20]. SI was similar to the Fisher's Discriminant Ratio (Rd) value measurement, which is a measure of the statistical separation between two populations using their means and standard deviations. In Zucker, et al. [20], the authors concluded that VSSC yielded smaller CVs and a greater SI compared with BSSC. This feature has proven useful in the analysis of microvesicles in biological samples [21, 22]. Observations show that the diameter of VLPs in aquatic samples falls mainly in the range of 20–200 nm. Among them, VLPs with a diameter of 30–70 nm account for more than 65% of the total [23]. Therefore, VLPs are about the same size as microvesicles or metal nanoparticles mentioned above. The aim of this paper is to test if VSSC would be useful for virioplankton detection in natural seawater samples.

2 | MATERIALS AND METHODS

2.1 | Sampling

Samples were collected at coastal and oceanic stations in the Western Pacific (Figure 1). For coastal stations, sampling was conducted from the 11th to 12th of September, 2017 onboard R/V "*Kejiao No.1*" in the Jiaozhou Bay, in the Yellow Sea at 4 stations (Stn. C1 to C4, C: abbreviation for coastal). Seawater samples were taken with 5 L Niskin bottles at 1 to 4 depths depending on the water column depth. For oceanic stations, samples were collected onboard the R/V "*Kexue*" in the tropical Western Pacific at 2 stations (Stn. O1 and O2, O: the abbreviation for oceanic) on August 1st 2017. Samples were collected at 11 different depths from the surface to about 2700 m. Sampling was performed using a CTD profiler (Sea-Bird SBE 9) with 10-L Niskin bottles. At each station, 2 samples of 4 ml of seawater were preserved with paraformaldehyde (1% final concentration) immediately after sampling, kept at room temperature in the dark for 15 min to allow the fixative to operate, and then freeze-trapped in liquid nitrogen until laboratory analysis onshore [24, 25].

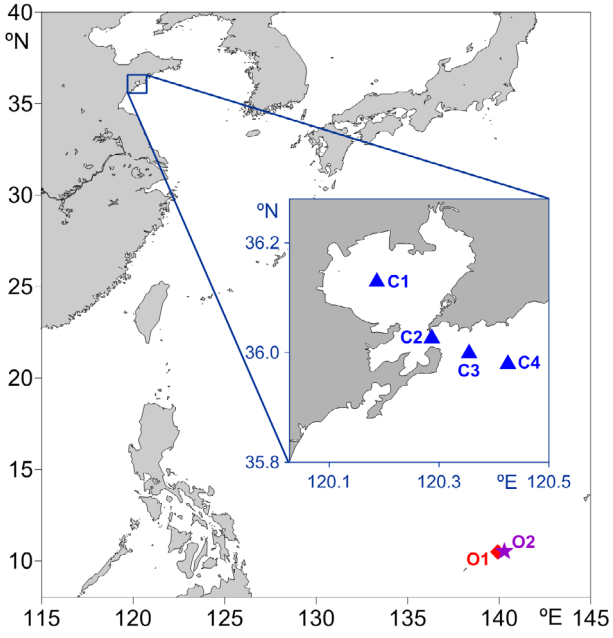


FIGURE 1 Sampling station. Stns. C1-C4: coastal stations, Stns. O1, O2: oceanic stations [Color figure can be viewed at wileyonlinelibrary.com]

2.2 | FCM counting

VLPs were determined by a CytoFLEX S flow cytometer (Beckman Coulter). The CytoFLEX S was equipped with violet (405 nm), blue (488 nm) and red (638 nm) lasers to detect up to 13 fluorescent channels. The CytoFLEX S used the technology of the Wavelength Division Multiplexer (WDM) used in the telecommunications industry to deconstruct and measure multiple wavelengths of light. This technology relies on fiber optics and band pass filters to separate the different light wavelengths. Unlike more conventional instruments, the multiple dichroic filters used to separate and direct the various light paths are not required. In addition, the WDM on the CytoFLEX S flow cytometer utilizes Avalanche Photodiode detectors (APD), instead of the photomultiplier tubes (PMT) found on most flow cytometers (refer to the Beckman Coulter brochure). APD have a better quantum efficiency than PMT in excess of 80%. [26]. Quantum efficiency, that is, the photon-electron conversion yield, is the number of the electron–hole carrier pairs generated per incident–absorbed photon. This higher photon-electron conversion yield reduces measurement error thus facilitating higher sensitivity and resolution. The CytoFLEX S features the capability to measure the side scatter of the violet as well as the blue laser beams. This increases the range of particles that can be detected as the smaller violet (405 nm) wavelength results in more orthogonal light scattering at any given particle size compared to the blue (488 nm) wavelength. To use VSSC to detect VLPs, the filter configuration from a regular CytoFLEX S was changed according to Zucker, et al. [20]: the 405 nm laser filter position 450/45 nm was changed to a 405/10 nm band-pass filter in order to collect the violet photons scattered by the particles. No additional small particles detector was employed in this study. There was no other special optical modification.

Fixed samples were thawed in the dark at room temperature and then filtered through a 100 μm mesh to remove large particles (in order to prevent any clogging). Filtered samples were 10-fold diluted in 0.22 μm filtered autoclaved TE buffer (Tris-EDTA, 100 mmol L^{-1} Tris–HCl, 10 mmol L^{-1} EDTA, pH = 8.0, Sigma) to reach an ideal working event rate (200–800 events s^{-1}) and to avoid electronic coincidences and thus a bias in counts. Diluted samples were stained with SYBR Green I (Molecular Probes Inc.) at a final concentration of $5*10^{-5}$ dilution of the commercial stock (v/v), vortexed for 15 s, incubated for 10 min in the dark at 80°C, and then cooled for 5 min prior to analysis [15, 27]. The trigger was set to green fluorescence signal, and VLPs could be identified on the basis of VSSC versus green fluorescence intensities. Data was collected in logarithmic mode thanks to the CytExpert software (v2.3.0.84, Beckman Coulter). For daily calibration of the CytoFLEX S, a solution of 2 μm fluorescent polystyrene beads (Polysciences) was used as the internal standard. In addition, to detect small changes in instrument performance that would affect submicron analysis, the use of fluorescent polystyrene beads (Megamix FSC & SSC Plus, BioCytex) in sizes of 0.1, 0.16, 0.2, 0.24, 0.3, 0.5, and 0.9 μm as described in Wisgrill, et al. [22] is also recommended for daily calibration of the flow cytometer (Figure S1). TE-buffer was pre-treated (blanks) and analyzed identically to samples.

As detection of coincidence (so-called "swarm") is a huge problem in small particle detection, the usual approach is to do serial dilution until the subpopulations of small particles remain stable with further dilutions. Additional analyses have been performed on both coastal and oceanic samples by doing serial dilutions (2, 10, 100, 1000 times) for each. The 2- and 1000- times dilutions were not usable because the subpopulations were either way too concentrated (leading to promiscuous clusters) or too diluted (no more cluster). However, the 10- and 100- times dilutions resulted in similar subpopulations of VLPs (See Figures S1 and S2).

2.3 | EFM counting

For EFM enumeration, a modification of the method of Noble and Fuhrman [16] was used. About 100 μl of the samples were diluted to 1 ml with 0.02 μm filtered Milli-Q water, then filtered onto a 0.02 μm anodisc filter (Whatman). Filters were placed on 100 μl of SYBR Green I solution (final dilution 2.5×10^{-3}, Molecular Probes), and stained for 20 min in the dark. After staining, excess dye was removed with Kimwipes (Kimberly–Clark). The filters were then mounted with 20 μl *p*-phenylenediamine (0.1% v/v) anti-fade mounting medium [9]. VLPs were counted using an epifluorescence microscope (BX51, Olympus; filter U-MWIB2) equipped with a microscope digital camera (DP80, Olympus). For each slide, 10–20 randomly chosen views were counted. At least 200 VLPs, distinguished on the basis of shape and brightness (Figure 3) [16], were counted for each slide.

2.4 | Statistical analysis

Flow cytometry data were analyzed with CytExpert software (Beckman Coulter). Statistical analysis and scientific graphing were conducted using Prism 7 software (GraphPad Software). Pearson correlation analysis and two independent-sample *t*-tests were used to compare the VLPs counts using different methods or parameters. SI was introduced to better prove the efficiency of using VSSC [28]. In this study, SI was calculated using the VSSC and BSSC median intensity and robust standard deviation (rSD) of VLPs and Non-VLPs (from Figure 4):

$$SI = (Median_{Non-VLPs} - Median_{VLPs}) / (2*rSD_{VLPs})$$

3 | RESULTS

3.1 | VLPs abundance and sub-clusters

The modification of the CytoFLEX S flow cytometer using a 405/10 nm filter made it possible to record the light scatter from the violet (405 nm) laser beam in addition to the conventional light scatter from the blue (488 nm) laser beam. VLPs could thus be simultaneously gated from bi-parametric plots of VSSC or BSSC versus SYBR Green I fluorescence (Figure 2A–C). Blanks consisting of TE-buffer were pre-

treated and analyzed identically to samples, further facilitating the recognition of VLPs from potential Non-VLPs (Figure 2D).

VLPs abundances in 11 coastal samples ranged from 6.65×10^6 particles ml^{-1} to 1.90×10^7 particles ml^{-1}, with a mean concentration of $5.60 \pm 1.72 \times 10^7$ particles ml^{-1} (Table S1). Up to 6 VLPs sub-clusters (V1–V6) corresponding to viruses displaying various fluorescence intensities could be identified (Figure 2A, E). V2 and V3 sub-clusters are the most abundant, accounting for 45.43% ± 2.89% and 25.43% ± 3.20% of VLPs, respectively.

In oceanic samples, VLPs abundances were about one order of magnitude lower than in coastal samples, ranging from 6.95×10^5 particles mL^{-1} (Stn. O1, 1000 m) to 4.00×10^6 particles mL^{-1} (Stn. O2, 75 m), with a mean concentration of 2.23×10^6 particles mL^{-1} (Table S2). For samples from the upper 75 m of the water column, 4 VLPs sub-clusters (V1, V2a, V2b, and V3) could be identified (Figure 2B, F). Below 100 m, the middle fluorescent sub-clusters, that is, V2a and V2b in Figure 2B merged into one single V2 sub-cluster, making a total of 3 VLPs sub-clusters (V1, V2, and V3) for these samples (Figure 2C, G).

3.2 | Control of FCM and EFM counts

EFM counts (Figure 3A) were performed for coastal samples to compare with the FCM counts. EFM results show that VLPs abundance was lower but on the same order of magnitude as FCM (Table S1), ranging from 1.81×10^7 particles ml^{-1} to 5.95×10^7 particles ml^{-1}, with a mean concentration of $3.30 \pm 1.20 \times 10^7$ particles ml^{-1}. As revealed by Pearson correlation analysis, FCM and EFM counts were significantly correlated (coefficient = 0.806, $p < 0.001$ using VSSC, and 0.698, $p < 0.001$ using BSSC, respectively), suggesting FCM using VSSC or BSSC is suitable for the enumeration of viruses (Figure 3B, C). However, FCM estimates of VLPs abundance were higher than EFM, by an average factor of 1.64 for VSSC and 1.83 for BSSC.

3.3 | Comparison of VSSC and BSSC

For the purpose of this study, VLPs abundance was determined for each datafile using both the BSSC and VSSC intensity versus SYBR Green I fluorescence distribution (Figure 4). For high VLPs abundance samples, sub-clusters could also be identified with the BSSC cytogram (Figure 4B) and was similar to the VSSC cytogram (Figure 4A). However, separation of VLPs from Non-VLPs (in gray on the histograms of Figure 4C and D) was greater on the VSSC cytogram than the BSSC cytogram. We observed some Non-VLPs overlap with low fluorescent VLPs sub-clusters (Figure 4B and D, F and H, J and L), indicating for a same datafile some overestimation of VLPs counts with BSSC. Indeed, counts based on BSSC were always higher than those performed with VSSC, for coastal samples (Figure 5A), by an average factor of 1.12, even though the difference was not significant ($p > 0.05$). For oceanic

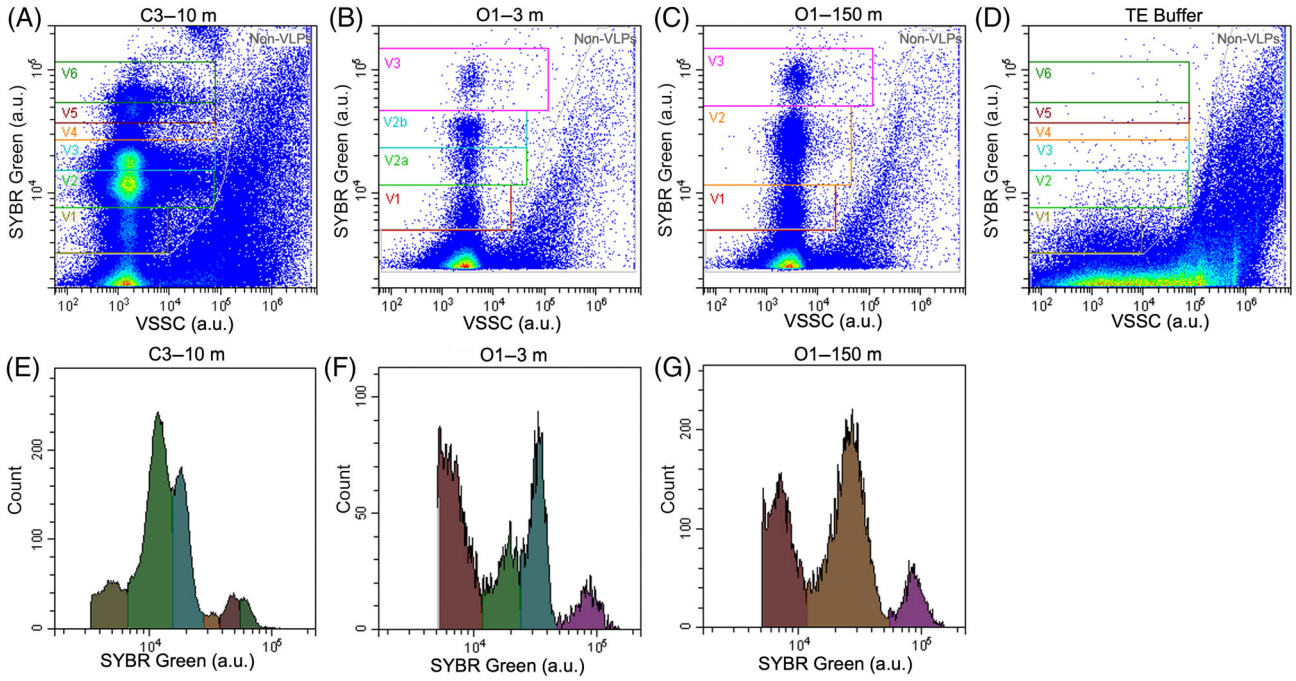


FIGURE 2 Cytograms and histograms of coastal (A, E) and oceanic (B, C, F, G) and TE buffer blank (D) samples. au: arbitrary units. Station name and sampling depth are marked on top of each plot. C, coastal stations and O, oceanic stations. VLPs sub-clusters are marked as V1, V2, and so on (numbers increase with the fluorescence intensity). Total VLPs equal the sum of all the sub-cluster events on the cytogram. (A–D) All events plotted. (E–G) Gate was set on VLPs only. Notice the threshold of coastal and oceanic samples is different, likely due to a different load in detritic particles [Color figure can be viewed at wileyonlinelibrary.com]

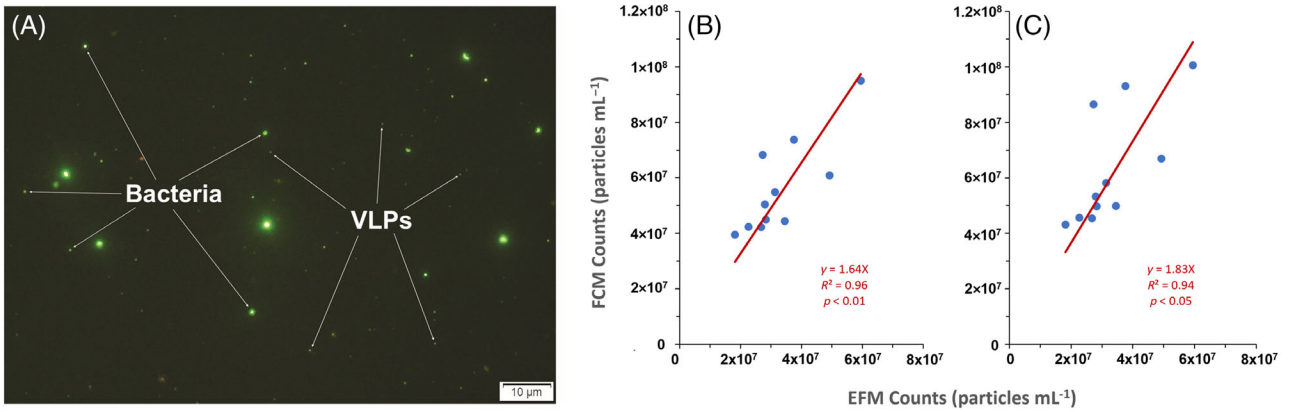


FIGURE 3 An epifluorescence micrograph (a) showing typical EFM counting and the relationship between VLPs counts by EFM and FCM (B and C). (A) Tiny green dots are identified as VLPs, while larger green dots are bacteria. (B) Linear regression of VLPs counts by EFM (*x*-axis) and FCM using violet side scatter (VSSC, *y*-axis). (C) Linear regression of VLPs counts by EFM (*x*-axis) and FCM using blue side scatter (BSSC, *y*-axis) [Color figure can be viewed at wileyonlinelibrary.com]

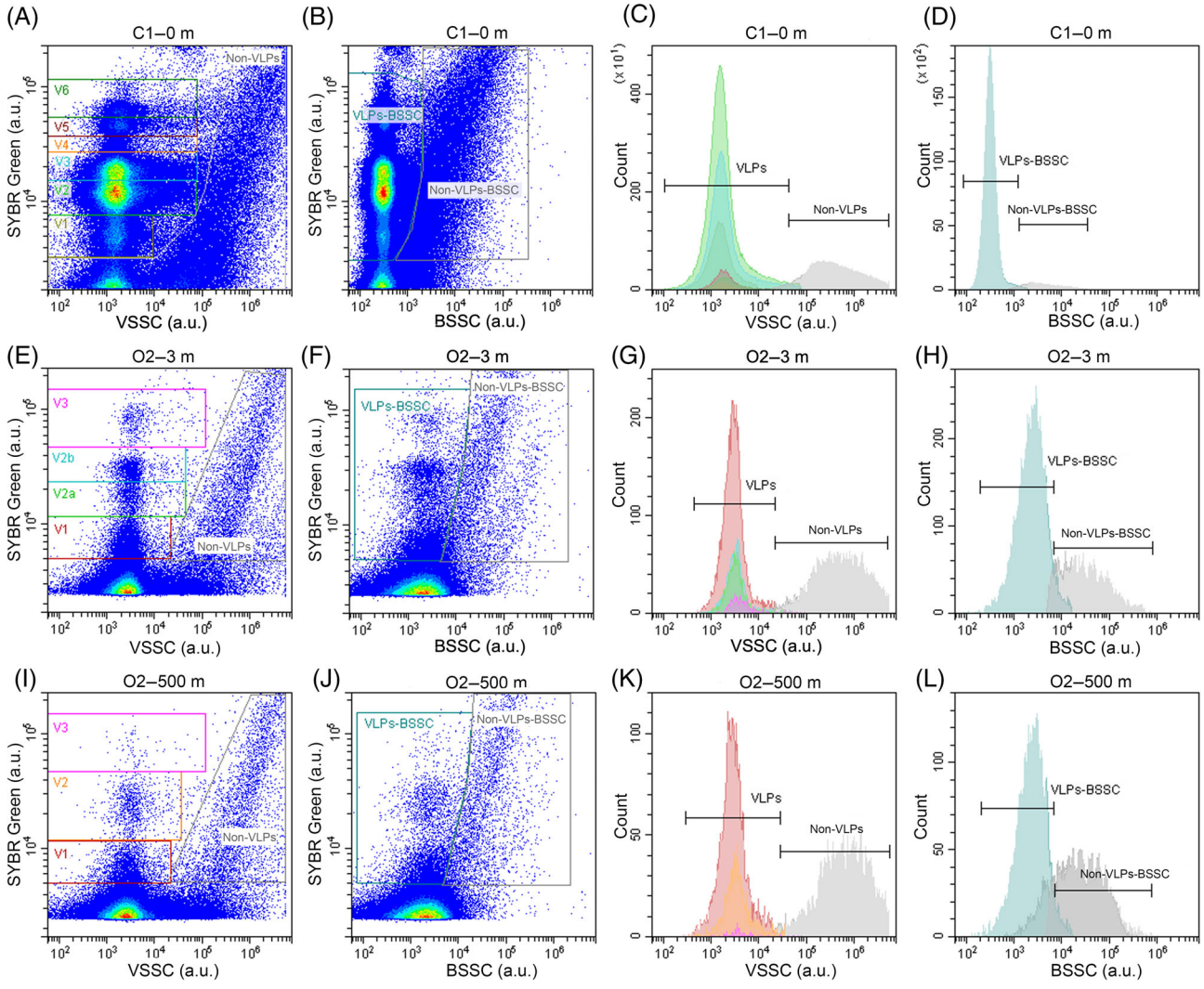


FIGURE 4 Comparison of violet side scatter (VSSC) and blue side scatter (BSSC) from coastal (A–D) and oceanic (E–L) samples. au: arbitrary units. The two columns on the left display SYBR Green induced fluorescence (au) versus either VSSC or BSSC: Regions show the different VLPs sub-clusters marked as V1, V2, and so on. Total VLPs equal the sum of all the sub-cluster events on the cytogram. The two columns on the right display histograms of VSSC or BSSC: Markers indicate the VLPs and the Non-VLPs. The various colors match the different VLPs regions defined on the cytograms of the 2 first columns. Station name and sampling depth are marked on top of each plot. (C) coastal stations, O: oceanic stations. For coastal samples (A–D), only 50% events were plotted. Notice the gain configuration and threshold of coastal and oceanic samples is different. [Color figure can be viewed at wileyonlinelibrary.com]

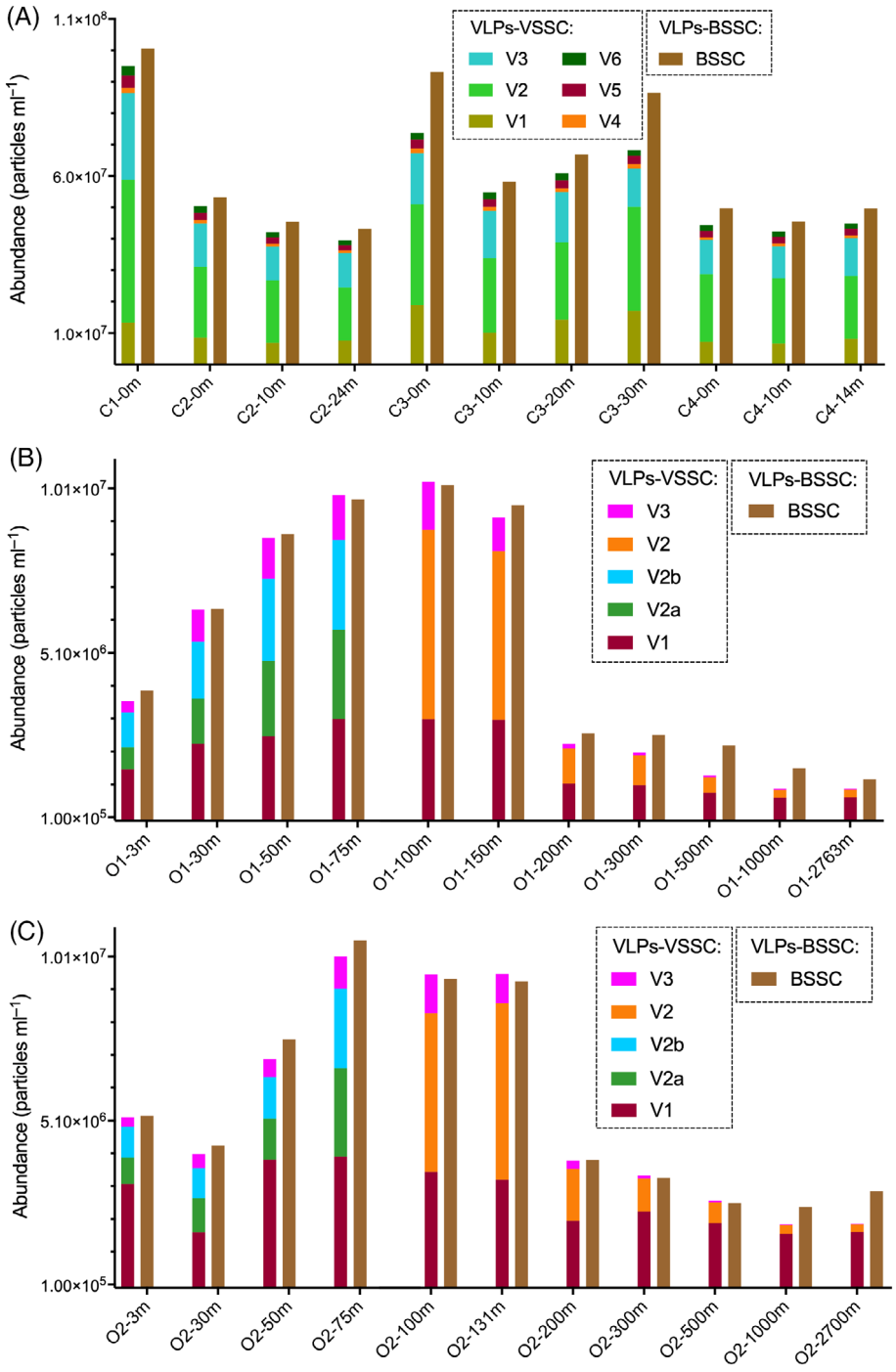


FIGURE 5 VLPs abundance (particles ml^{-1}) counted using VSSC and BSSC from coastal (A) and oceanic (B, C) samples. Sample names are marked on the x-axis of each plot, in the form of station name-sampling depth. C, coastal stations and O, oceanic stations. VLPs sub-clusters are marked as V1, V2, and so on. For coastal samples, VSSC counted abundance = V1 + V2 + V3 + V4 + V5 + V6. For oceanic sample of 3–75 m depth, VSSC counted abundance = V1 + V2a + V2b + V3. For other oceanic samples, VSSC counted abundance = V1 + V2 + V3 [Color figure can be viewed at wileyonlinelibrary.com]

samples, the optical resolution of various sub-clusters using BSSC was less clear (Figure 4F and J). Especially for deep sea samples, it's difficult to distinguish low fluorescent VLPs from Non-VLPs (Figure 4L, 500 m depth). BSSC counts were also higher than VSSC (Figure 5B and C), by an average factor of 1.03 for samples in the upper 200 m water column and 1.45 for deep sea samples, respectively. But neither difference was statistically significant ($p > 0.05$). To better prove the efficiency of using VSSC, the SI was calculated with the VSSC and BSSC median intensity and robust standard deviation of VLPs and Non-VLPs according to de Rond et al. [28]. The SI thereby is a measure for the separation between VLPs subpopulations and the Non-VLPs. Figure 6 evidences that for all the samples, both coastal and

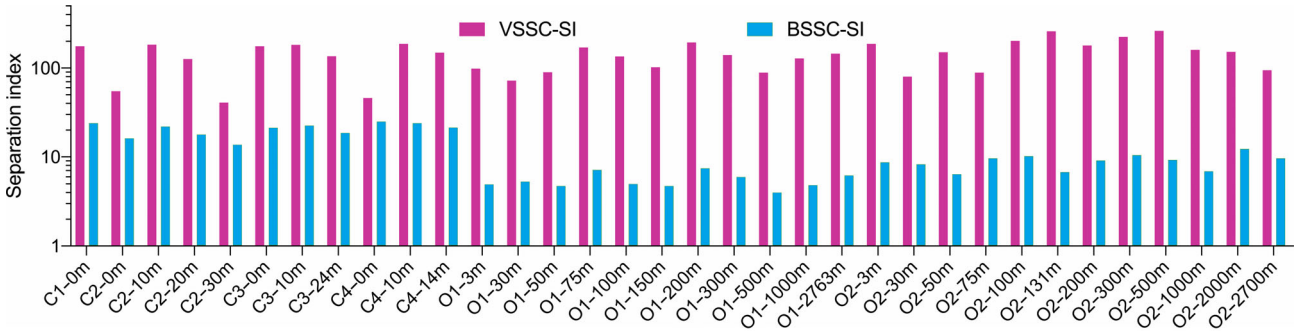


FIGURE 6 Separation index (SI) calculated for all samples in this study using the VSSC and BSSC median intensity and robust standard deviation (rSD) of VLPs and non-VLPs (from Figure 4). $SI = {}^{(Median_{Non-VLPs} - Median_{VLPs})}/_{(2*rSD_{VLPs})}$. Sample names are marked on the *x*-axis, in the form of station name-sampling depth. C, coastal stations, O, oceanic stations [Color figure can be viewed at wileyonlinelibrary.com]

open ocean, the SI of VSSC is superior to BSSC by a factor ranging from 1.84 to 38.57 (Table S3). Our results show that VSSC is a better variable than BSSC regarding VLPs counting, especially for low VLPs abundant samples.

4 | DISCUSSION

For many laboratories, FCM has become the routine method for quantifying VLPs in aquatic systems because of its high reproducibility, high sample throughput, and ability to distinguish several subclusters of VLPs [15]. The conventional procedure of VLPs FCM enumeration uses the bi-parametric plot of BSSC vs fluorescence from DNA-binding stains [15, 24]. However, the majority of flow cytometers are not built for the purpose of detecting nano-sized particles such as viruses. Due to their small size and low nucleic acid content, sometimes it's difficult to separate VLPs signals from the Non-VLPs of the sample. One way to solve this problem is to modify the cytometers with high-powered lasers (to get more photons scattered), higher voltage photomultipliers (to amplify the signal), or implement an extra small-particle detector [29], but all of these modifications can be expensive and are not available on all flow cytometers.

The 405 nm laser has become common on commercially available cytometers. Research based on the Mie light scatter theory have proved that 405 nm VSSC could generate significantly better light scatter signals than the 488 nm BSSC, increasing the precision and resolution over instrument noise for nanoparticles or microvesicles detection [20–22]. Indeed, McVey et al [21] have clearly demonstrated that side scatter for 405 nm photons is superior to the one for 488 nm photons for the detection of small (100–500 nm) spherical particles. Because the amount violet (405 nm) photons scattered at 90° is twice as important as the blue (488 nm) photons, the signal measured by flow cytometry is better for the VSSC. However, the quantum efficiency of the avalanche photodiode is actually twice as high (about 80%) for the 488 nm photons as that of the 405 nm photons (about 40%) [26]. In addition, using shorter wavelength light increases the instrument's resolving power of similarly sized particles (Abbe's Law), because the light scattered at lower wavelengths is less diffused. That is why the optical resolution of the various VLPs clusters looks better (lower CVs) with the 405 nm than the 488 nm laser beam (Figure 4).

This article aims to describe how the use of VSSC can better characterize, and count VLPs in natural seawater samples. We have demonstrated that the use of VSSC along with a slight modification to the CytoFLEX S flow cytometer is suitable for enumeration of viruses from various natural aquatic samples (in coastal or open ocean, from the surface or deeper). The SI calculated both for BSSC and VSSC quantifies the better separation between VLPs subpopulations and Non-VLPs when using the VSSC. As such, we have demonstrated that VSSC increased the capacity to resolve VLPs over instrument and sample Non-VLPs, making it easier to gate VLPs events on cytograms and eliminating some Non-VLPs overlapping with VLPs when gated on the BSSC. The VLPs abundance we obtained were around 10^7 particles ml^{-1} for coastal and 10^6 particles ml^{-1} for oceanic samples. These results are in the range of viral abundance reported in the literature for similar environments [23]. VLPs abundance acquired using VSSC are highly correlated with those obtained with BSSC, but more accurate as some Non-VLPs has not been considered anymore, proving VSSC is reliable. The counts performed by EFM were in the same order of magnitude than flow cytometry, they are however lower than expected (by a factor 1.64 compared to VSSC counts and a factor 1.83 compared to BSSC counts). After staining the sample, 10–20 randomly chosen views were imaged and then analyzed. VLPs were distinguished and counted on the basis of shape, size, and brightness (green intensity induced by SYBR Green I dye) from the picture. We were unable to provide any explanation for that discrepancy in counts and no other fluorescence methods were evaluated to confirm, definitively, the presence and amount of viruses using EFM. As described in Kaletta et al., the complex and heterogeneous nature of environmental water samples, together with a background rather high in abiotic particles, presents challenges to accurate virus quantification [30]. Interestingly, none of the methods tested in Kaletta et al. [30] was able to provide reliable accurate absolute values, as the exact concentration of the viral particles in these samples is virtually impossible to determine. All non-targeted methods such as FCM and EFM used in this study and Kaletta et al. [30], or nanoparticle tracking analysis

(NTA) used in Kaletta et al. [30] could only resolve particles based on nucleic acid stains but not the particles themselves. All methods have the potential for inaccuracies, that is, through the erroneous quantification of small bacteria or extracellular vesicles as described in Breitbart et al. [31]. That is why the term VLPs as "virus-like-particles" rather than viruses *sensus stricto* was used for the flow cytometry analyses in this study. EFM has been used extensively in the literature to count VLPs [23, 29]. Before the invention of automated thresholding approach, scientists could separate and count VLPs under EFM by direct visualization (naked eyes) and manual counting. In this research, no automated thresholding approach was employed. Instead, we used an epifluorescent microscope equipped with a camera (instead of naked eye), and performed a manual counting directly from the images, just as a control to see if the abundances obtained by two counting methods were within the same range of values. This is the case, and the lower EFM counts do not impact the aim of this article as flow cytometry data are self-sufficient to demonstrate the improvement in the VLPs optical resolution using VSSC rather than BSSC.

Another important feature of this study is that the 405 nm laser beam helps to eliminate some of the background noise. Indeed, in natural samples, BSSC detection of small viruses, that is, with low nucleic acid dye fluorescence, may overlap with Non-VLPs (Figure 4), and cause some errors in VLPs abundance estimations. When compared to BSSC, VSSC improves the optical resolution and thus the precision in the detection of VLPs against Non-VLPs, for both coastal and oceanic samples (Figure 4). One can notice that the Non-VLPs is different between coastal and oceanic samples (Figure 2). This is likely due to a different load in very small materials (debris, dissolved organic matter) that can be either autofluorescent or pass within the laser beams with some free SYBRGreen molecules around them (SYBR Green is hydrophobic).

To summarize, the use of VSSC does increase the accuracy of VLPs abundance estimation in natural marine samples, which is critical in virus ecology research in order to understand the role of VLPs in the functioning of the ecosystem.

The innovation of using VSSC on the new generation of flow cytometer that is equipped with avalanche photodiodes, allows for a simple, low cost, yet more accurate strategy to enumerate VLPs from aquatic samples, especially for low virioplankton abundance environments.

AUTHOR CONTRIBUTIONS

Yuanchu Zhao: Data curation (equal); formal analysis (equal); investigation (equal); validation (equal); visualization (equal); writing – review and editing (equal). **Yuan Zhao:** Conceptualization (equal); data curation (equal); formal analysis (equal); funding acquisition (equal); investigation (equal); visualization (equal); writing – original draft (lead); writing – review and editing (equal). **Shan Zheng:** Data curation (equal); investigation (equal); methodology (equal); resources (equal); visualization (equal); writing – review and editing (equal). **Li Zhao:** Data curation (equal); formal analysis (equal); validation (equal); writing – review and editing (equal). **Wuchang Zhang:** Funding acquisition (equal); project administration (equal); resources (equal); writing – review and editing (equal). **Tian Xiao:** Project administration (equal); resources (equal); writing – review and editing (equal). **Gérald J Grégori:** Conceptualization (equal); data curation (equal); funding acquisition (equal); supervision (equal); writing – original draft (equal); writing – review and editing (equal).

ACKNOWLEDGMENTS

This study was funded by the National Natural Science Foundation of China (No. 42076139), the Open Fund of Pilot National Laboratory for Marine Science and Technology (Qingdao) (No. QNLM20160RP0311), the CNRS-NSFC Joint Research Projects Program (CNRS-272110, NSFC 41711530149), the 2017-2019 Sino-French Cai Yuanpei Program and the International Research Project-Dynamics and Function of Marine Microorganisms (IRP-DYF2M): insight from physics and remote sensing, CNRS-CAS. Special thanks to the great efforts of the crew of R/V "*Kejiao No.1*" during the cruise in Jiaozhou Bay, and R/V "*Kexue*" during the cruise in the tropical western Pacific, respectively. We also thank Olivier Jaen for his support.

CONFLICT OF INTEREST

The authors declare that they have no conflict of interest.

PEER REVIEW

The peer review history for this article is available at https://publons.com/publon/10.1002/cyto.a.24674.

DATA AVAILABILITY STATEMENT

All data has been uploaded to flowrepository.org (http://flowrepository.org/id/FR-FCM-Z56X).

ORCID

Yuan Zhao https://orcid.org/0000-0002-8892-2100
Wuchang Zhang https://orcid.org/0000-0001-7534-8368
Gérald Grégori https://orcid.org/0000-0003-1645-9468

REFERENCES

1. Suttle CA. Viruses in the sea. Nature. 2005;437:356–61.
2. Weinbauer MG. Ecology of prokaryotic viruses. FEMS Microbiol Rev. 2004;28:127–81.
3. Weinbauer M, Bettarel Y, Cattaneo R, Luef B, Maier C, Motegi C, et al. Viral ecology of organic and inorganic particles in aquatic systems: avenues for further research. Aquat Microb Ecol. 2009;57:321–41.
4. Wommack KE, Nasko DJ, Chopyk J, Sakowski EG. Counts and sequences, observations that continue to change our understanding of viruses in nature. J Microbiol. 2015;53:181–92.
5. Bergh Ø, Børsheim KY, Bratbak G, Heldal M. High abundance of viruses found in aquatic environments. Nature. 1989;340:467–8.
6. Børsheim KY, Bratbak G, Heldal M. Enumeration and biomass estimation of planktonic bacteria and viruses by transmission electron microscopy. Appl Environ Microbiol. 1990;56:352–6.
7. Proctor LM, Fuhrman JA. Viral mortality of marine bacteria and cyanobacteria. Nature. 1990;343:60–2.
8. Suttle CA, Fuhrman JA. Enumeration of virus particles in aquatic or sediment samples by epifluorescence microscopy. In: Wilhelm SW,

Weinbauer MG, Suttle CA, editors. Manual of aquatic viral ecology. Waco, TX: American Society of Limnology and Oceanography; 2010. p. 145–53.
9. Patel A, Noble RT, Steele JA, Schwalbach MS, Hewson I, Fuhrman JA. Virus and prokaryote enumeration from planktonic aquatic environments by epifluorescence microscopy with SYBR green I. Nat Protoc. 2007;2:269–76.
10. Olson R, Vaulot D, Chisholm S. Marine phytoplankton distributions measured using shipboard flow cytometry. Deep Sea Res Part A Oceanogr Res Papers. 1985;32:1273–80.
11. Yentsch CM, Horan PK, Muirhead K, Dortch Q, Haugen E, Legendre L, et al. Flow cytometry and cell sorting: a technique for analysis and sorting of aquatic particles. Limnol Oceanogr. 1983;28: 1275–80.
12. Chisholm SW, Olson RJ, Zettler ER, Goericke R, Waterbury JB, Welschmeyer NA. A novel free-living prochlorophyte abundant in the oceanic euphotic zone. Nature. 1988;334:340–3.
13. Lomas MW, Bronk DA, Van den Engh G. Use of flow cytometry to measure biogeochemical rates and processes in the ocean. Ann Rev Mar Sci. 2011;3:537–66.
14. Marie D, Simon N, Guillou L, Partensky F, Vaulot D. Flow cytometry analysis of marine picoplankton. In: Diamond RA, DeMaggio S, editors. Living Color: Protocols in Flow Cytometry and Cell Sorting. New York, NY: Springer-Verlag Berlin Heidelberg; 2000. p. 421–54.
15. Brussaard CP, Payet JP, Winter C, Weinbauer MG. Quantification of aquatic viruses by flow cytometry. In: Wilhelm SW, Weinbauer MG, Suttle CA, editors. Manual of aquatic viral ecology. Waco, TX: American Society of Limnology and Oceanography; 2010. p. 102–9.
16. Noble RT, Fuhrman JA. Use of SYBR green I for rapid epifluorescence counts of marine viruses and bacteria. Aquat Microb Ecol. 1998;14: 113–8.
17. Magiopoulos I, Pitta P. Viruses in a deep oligotrophic sea: seasonal distribution of marine viruses in the epi-, meso- and bathypelagic waters of the eastern Mediterranean Sea. Deep-Sea Res I Oceanogr Res Pap. 2012;66:1–10.
18. Payet JP, Suttle CA. Physical and biological correlates of virus dynamics in the southern Beaufort Sea and Amundsen gulf. J Mar Syst. 2008;74:933–45.
19. Winter C, Kerros M-E, Weinbauer MG. Seasonal and depth-related dynamics of prokaryotes and viruses in surface and deep waters of the northwestern Mediterranean Sea. Deep-Sea Res I Oceanogr Res Pap. 2009;56:1972–82.
20. Zucker RM, Ortenzio JNR, Boyes WK. Characterization, detection, and counting of metal nanoparticles using flow cytometry. Cytometry A. 2016;89A:169–83.
21. McVey MJ, Spring CM, Kuebler WM. Improved resolution in extracellular vesicle populations using 405 instead of 488 nm side scatter. J Extracell Vesicles. 2018;7:1454776.
22. Wisgrill L, Lamm C, Hartmann J, Preißing F, Dragosits K, Bee A, et al. Peripheral blood microvesicles secretion is influenced by storage time, temperature, and anticoagulants. Cytometry A. 2016;89A: 663–72.
23. Wommack KE, Colwell RR. Virioplankton: viruses in aquatic ecosystems. Microbiol Mol Biol Rev. 2000;64:69–114.
24. Marie D, Brussaard CP, Thyrhaug R, Bratbak G, Vaulot D. Enumeration of marine viruses in culture and natural samples by flow cytometry. Appl Environ Microbiol. 1999;65:45–52.
25. Marie D, Partensky F, Vaulot D, Brussaard C. Enumeration of phytoplankton, bacteria, and viruses in marine samples. Curr Protoc Cytom. 1999;10:11.11.1–11.11.15.
26. Lawrence WG, Varadi G, Entine G, Podniesinski E, Wallace PK. A comparison of avalanche photodiode and photomultiplier tube detectors for flow cytometry. Proc SPIE 6859, imaging, Manipulation, and Analysis of Biomolecules, Cells, and Tissues. 2008; VI, 6890M.
27. Brussaard CP. Optimization of procedures for counting viruses by flow cytometry. Appl Environ Microbiol. 2004;70:1506–13.
28. De Rond L, Van der Pol E, Bloemen PR, Van Den Broeck T, Monheim L, Nieuwland R, et al. A systematic approach to improve scatter sensitivity of a flow cytometer for detection of extracellular vesicles. Cytometry A. 2020;97:582–91.
29. Zamora JLR, Aguilar HC. Flow Virometry as a tool to study viruses. Methods. 2018;134-135:87–97.
30. Kaletta J, Pickl C, Griebler C, Klingl A, Kurmayer R, Deng L. A rigorous assessment and comparison of enumeration methods for environmental viruses. Sci Rep. 2020;10:18625.
31. Breitbart M, Bonnain C, Malki K, Sawaya NA. Phage puppet masters of the marine microbial realm. Nat Microbiol. 2018;3:754–66.

SUPPORTING INFORMATION

Additional supporting information can be found online in the Supporting Information section at the end of this article.

How to cite this article: Zhao Y, Zhao Y, Zheng S, Zhao L, Zhang W, Xiao T, et al. Enhanced resolution of marine viruses with violet side scatter. Cytometry. 2022. https://doi.org/10.1002/cyto.a.24674